THE JOURNAL OF COMPARATIVE NEUROLOGY 407:65–76 (1999)

Kainate Activation of Horizontal, Bipolar, Amacrine, and Ganglion Cells in the Rabbit Retina

ROBERT E. MARC*
John Moran Eye Center, University of Utah School of Medicine, Salt Lake City, Utah 84132

ABSTRACT

Patterns of excitation in populations of retinal bipolar, amacrine, and ganglion cells were mapped by activating α-amino-3-hydroxyl-5-methylisoxazole-4-propionic acid (AMPA) and kainate (KA) receptors with KA in the presence of the channel-permeant guanidinium analogue 1-amino-4-guanidobutane (AGB). Registered serial thin sections were probed with immunoglobulins targeting AGB, glutamate, glycine, and γ-aminobutyric acid (GABA) to visualize KA-evoked responses and the neurochemical signatures of distinct cell types. OFF-center cone bipolar cells and both type A and type B horizontal cells were strongly activated by KA. ON-center cone bipolar cells displayed weak AGB signals that arose at least partially, if not entirely, from coupling with KA-responsive glycinergic amacrine cells, whereas rod bipolar cells exhibited no detectable AGB permeation after KA activation. GABA-positive amacrine cells displayed a range of KA responses, some possessing little AGB signal even after strong KA activation, whereas all identifiable glycine-positive amacrine cells were driven by KA. Quantitative agonist responsivities of cells in the ganglion cell layer revealed that starburst amacrine cells are the most KA-responsive cell type in that layer. Ganglion cells varied in KA responsivity across morphologic subtypes, with a large α-like ganglion cell group the being the most KA responsive. Some ganglion cells displayed weak KA responses, even with saturating doses, that may have been be due to an absence of AMPA/KA receptors or to the existence of AGB-impermeant AMPA/KA receptor complexes. J. Comp. Neurol. 407:65–76, 1999.

Indexing terms: α-amino-3-hydroxyl-5-methylisoxazole-4-propionic acid receptors; kainate receptors; glycine; γ-aminobutyric acid

The organic cation 1-amino-4-guanidobutane (AGB) permeates ion channels activated by glutamate binding, and its accumulation in activated neurons can be detected immunocytochemically. Different types of retinal neurons appear to express varied mixtures of α-amino-3-hydroxyl-5-methylisoxazole-4-propionic acid (AMPA), kainic acid (KA), and N-methyl-D-aspartate (NMDA) receptors, and these mixtures may influence stimulus detection thresholds and visual response dynamic ranges. Many more retinal cell types have been described by using anatomical techniques than by using physiological techniques, and detailed comparisons of responses activated by glutamate agonists across comprehensive populations of cell types are not available. This report demonstrates that KA-evoked responses of mixed neuronal populations can be analyzed within single preparations, revealing differences in KA effectiveness across cell types and homogeneous responses within cell types.

The rigid glutamate analogue KA activates AMPA receptors in a nondesensitizing mode and activates KA receptors with rapid desensitization (Lerma et al., 1993; Paternain et al., 1995). Because AGB permeation reports the integrated entry of cations through an activated channel, its signal will disproportionately reveal AMPA receptors, although bona fide KA receptors are known to exist in the vertebrate retina (Hughes et al., 1992; Müller et al., 1992; Morigawa et al., 1995; Peng et al., 1995; Brandstätter et al., 1997). Even with this bias toward nondesensitizing activations, differences in the ability of KA to trigger AGB permeation in different cell types reveals that their glutamate receptor mixtures cannot be identical.

To make the case that a response reveals differences across cell types, one must demonstrate that at least some

Grant sponsor: National Institutes of Health; Grant number: EY02576.

*Correspondence to: Robert E. Marc, John Moran Eye Center, University of Utah School of Medicine, 75 N. Medical Drive, Salt Lake City, UT 84132. E-mail: robert.marc@hsc.utah.edu

Received 20 February 1998; Revised 11 November 1998; Accepted 1 December 1998

responses are homogeneous (i.e., quantitatively consistent) within an identifiable group of cells. This has not been achieved electrophysiologically, because cells necessarily must be recorded one by one, but it is quite possible with AGB mapping, especially when combined with neurochemical markers. This paper reports simultaneous comparisons of KA-activated responses in type A and type B horizontal cells, OFF-center and ON-center cone bipolar cells, rod bipolar cells, two broad groups of glycinergic amacrine cells, at least three groups of γ-aminobutyric acidergic (GABAergic) amacrine cells, including starburst amacrine cells, and three varieties of ganglion cells.

MATERIALS AND METHODS

Isolated retinal preparations

Adult male and female albino and pigmented rabbits were tranquilized with intramuscular ketamine/xylazine, deeply anesthetized with intraperitoneal urethane in saline, and killed by thoracotomy, all in accordance with institutional animal care and use guidelines. Both eyes were rapidly removed, and isolated retina pieces were prepared as described previously (Marc, 1999; Marc and Liu, 1985). Sets of retinal chips were incubated as matched series for 10 minutes in 100 μl droplets of Ames medium containing 5 mM AGB plus various KA doses. The data reported here came from the same population of samples described in the accompanying paper (Marc, 1999).

Specimen preparation and immunocytochemical visualization

Specimens were processed as described previously, serially sectioned in the horizontal plane at 250 nm onto 12-spot Teflon-coated slides (Cel-Line, Newfield, NJ), and probed with anti-AGB, anti-glutamate, anti-GABA, anti-glycine, anti-glutamine, and anti-glutathione immunoglobulins (IgGs) (Signature Immunologics Inc., Salt Lake City, UT; the author is a principal of Signature Immunologics Inc.).

Image analysis

Quantitative images of immunoreactivity were captured as described previously with fixed CCD camera gain and gamma in which gray value (GV) scales linearly with log concentration over a 2 log unit range. Calculations of the limits of IgG binding to surface targets show that the operating range of postembedding immunocytochemistry is from ≈50 μM to 13 mM, beyond which no further IgG binding can be accommodated sterically (Marc, unpublished data). Silver visualization produces density-scaled images, and linear image inversion produces intensity-scaled images. Serial images were aligned to within 250 nm rms error by conventional first-order image registration algorithms (PCI Remote Sensing, Richmond Hill, Ontario, Canada) with or without mosaicking. K-means pattern recognition classifications and data explorations were performed on registered, inverted images by using applications written in IDL (Research Systems Inc., Boulder, CO) by R. Murry of the University of Utah. An overview of and reference lists for pattern recognition methods are summarized in the report by Marc et al. (1995). In brief, common points on registered images are equivalent to lists of signals linked to a spatial position; K-means clustering methods separate statistical classes from these lists, and probability density histograms are extracted from the theme classes. Statistical separability indicates that the means and covariances for a set of N-dimensional data allows classifying a sample of those data into distinct classes. The probability of error (P_e) in classification is estimated from the transformed divergences of the classes assuming equal a priori probability densities (for a discussion of transformed divergence and P_e, see Marc et al., 1995). Most cell classes described herein were separable with $P_e \leq 0.01$, except where noted otherwise. Separable classes are also inherently statistically significant classes ($P \ll 0.01$). Sizes of cells were measured from calibrated grids superimposed on images and were not corrected for shrinkage.

Homogeneity of responses was judged as the width of a normalized AGB response histogram. Narrow, broad, and multimodal AGB response histograms are easily distinguished. Patches of classified cells often appeared to form regular arrays, and these were characterized numerically by their conformity ratios (the ratio of the class mean nearest-neighbor distance to its standard deviation). The statistical significance of the conformity ratio as a deviation from that predicted for a random pattern was determined from the conformity ratio "ready-reckoner" of Cook (1996).

Agents and sources

Ames medium was either purchased from Sigma-Aldrich Corp. (St. Louis, MO) or made according to Ames and Nesbett (1981) and supplemented with 5 mM AGB (agmatine sulfate; Sigma-Aldrich). KA was obtained from Research Biochemicals International (Natick, MA).

Figure preparation

All images are digital and were assembled from the raw data captured by CCD camera (see Image analysis, above). Selected frames of raw Tagged Image Format files were extracted for display, each was sharpened by unsharp masking, and, after entire images were assembled as a single figure, contrasts were adjusted with linear remapping to correct for out-of-gamut effects during printing. On large mosaics, occasional defects, such as cracks, folds, or dirt, were removed prior to classification by excision and replacement with neighboring background pixels. All final images were prepared in Adobe PhotoShop (version 4.0; Adobe Systems, Mountain View, CA).

RESULTS

The diversity of cell types in the inner nuclear layer (Strettoi and Masland, 1995) complicates interpretations of AGB response patterns. Do responses viewed in vertical sections represent stable but differing patterns of permeation into different cell types or intercellular variability within cell types? The combination of horizontal thin sections, image registration, amino acid immunoreactivity, KA-activated AGB signals, and pattern recognition provides evidence that intercellular variations arise from unique subpopulations of neurons with stable but differing KA responsivities.

KA activation in horizontal and bipolar cells

In the presence of a strong but subsaturating dose of KA, a diverse pattern of AGB signals appears in the distal half of the inner nuclear layer (Fig. 1). Some cells display strong AGB signals, some posses weaker but distinct

signals, and other parts of the image appear empty. The underlying cell types can be identified by extracting characteristic signatures. For example, ON-center cone bipolar cells can be discriminated from all other glutamate-rich bipolar cells by their glycine signals (Cohen and Sterling, 1986; Pourcho and Goebel, 1987; Kalloniatis et al., 1996). All rabbit horizontal cells contain elevated glutathione (Pow and Crook, 1995; Marc, unpublished data) and high glutamate levels. Rabbit type B horizontal cells have an elevated glutamine content (Marc, unpublished data). Müller cells are characteristically deficient in glutamate and glycine but have a strong glutamine signal and a modest glutathione signal.

All four metabolite signals can be combined with the KA-activated AGB signal in a five-dimensional clustering, revealing statistically separable groups of cells. Viewing the AGB signal alone (Fig. 1A) reveals that 43% of the retinal space lacks any KA-activated signal. If the data are viewed as a color triplet encoding glycine signals as red, AGB as green, and glutamate as blue (glycine · AGB · glutamate → red-green-blue [rgb] mapping), then the unresponsive space clearly is comprised of two cell groups: some type of glutamate-rich bipolar cell (pure blue cells in Fig. 1B) and Müller cells.

This is only one of the 20 unique data triplets possible with five signals, and it is not practical to display or attempt unaided visual interpretation of such image arrays. Pattern recognition solves this problem by defining unique cell groups based on their statistical properties and creating a theme map of those statistical groups. In Figure 1C, six unique populations emerge: type A horizontal cells, type B horizontal cells, rod bipolar cells, OFF-center bipolar cells, ON-center bipolar cells, and Müller cells. Two basic measures of each population can be extracted from pattern recognition analysis. First, the cells of a single theme class have characteristic mean AGB, glycine, and glutamate signal values that are visualized as different image densities or brightnesses (Fig. 1A,B). Second, the variances of amino acid and AGB signals differ across classes. Although this cannot be discerned by examining images, it can be displayed in probability density histograms.

The quantitative features of these cell types may be displayed as a signature matrix (Fig. 2) composed of a probability density histogram for each signal type (columns) and each cell type (rows). The y-axis of each histogram denotes the peak normalized probability of encountering a given amino acid or AGB concentration in a cell type. The x-axis represents the range of detectable intracellular concentrations (0.1–10 mM on a log scale). The alignment of the histogram peak on the x-axis indicates the modal concentration for that cell type. The width of the histogram indicates the range of possible concentrations of an amino acid or of AGB in that cell type, and the dispersion of signals indicates the homogeneity of the KA response for that type. Exposure to 30 μM KA induces strong AGB signals in horizontal cells and in a subset of bipolar cells. The width of the AGB response histogram is very narrow in horizontal cells, which indicates that they possess homogeneous KA responsivities. ON-center cone bipolar cells, which are identified by their distinctive glycine contents, have a bimodal response to KA, ranging from very weak to moderate. One class of bipolar cells has no response to KA and can be identified indirectly as rod bipolar cells (see below). By exclusion, the remaining cells are OFF-center cone bipolar cells, which exhibit strong heterogeneous responses to KA, as evidenced by their broad AGB histogram. Multiple morphologic subtypes of mammalian ON-center and OFF-center cone bipolar cells exist (Famiglietti, 1981; Wässle and Boycott, 1991; Mills and Massey, 1992; Euler and Wässle, 1995), and the broad KA response histograms for each of these cell types shows that the mechanisms of AGB permeation cannot be identical across subtypes within each class.

The patterns and sizes of cells classified in Figure 1 similarly indicate that ON-center and OFF-center cone bipolar cell populations represent mixed subtypes, whereas the rod bipolar cells represent a singular population. The distributions of type B horizontal cells and rod bipolar cells are regular. Nearest-neighbor spacing measurements yield a conformity ratio (also known as a "regularity index"; however, see Cook, 1996) of 3.6 for type B horizontal cells (n = 25) and 3.0 for rod bipolar cells (n = 50), characteristic of regularly distributed singular cell types (Wässle and Reimann, 1978; Vaney, 1985; Mills and Massey, 1991). Both ratios are significant at $P < 0.001$. Conversely, ON-center and OFF-center cone bipolar cells have conformity ratios of 1.1 and 1.3, respectively, suggesting that their patterning arises from uncorrelated superposition of several independent mosaics. In fact, these ratios are actually lower than is characteristic of random distributions, which suggests that some clustering is present. Finally, the soma diameters for each class are as follows: type B horizontal cells, 16.1 ± 1.0 μm (mean ± 1 S.D.; n = 9); rod bipolar cells, 11.3 ± 1.8 μm (n = 36); ON-center cone bipolar cells, 9.1 ± 2.4 μm (n = 67); and OFF-center cone bipolar cells, 9.2 ± 3.7 μm (n = 87). The type B horizontal cells and rod bipolar cells are significantly different from all other cells ($P < 0.01$ and $P < 0.026$, respectively; Student's t-test), but the cone bipolar cell sizes are indistinguishable from one another. Cone bipolar cells also have larger size variances, again implying that each population is composed of subtypes.

The identities of horizontal cells and ON-center cone bipolar cells are unambiguous, but the data in Figure 1 alone do not permit identification of the KA-unresponsive group as rod bipolar cells, although they are a unique statistical class. The axon terminals of rod bipolar cells can be visualized as arrays of strongly glutamate-positive elements in horizontal sections of the border between the inner plexiform layer and the ganglion cell layer (Fig. 3A). KA activation of AGB permeation is restricted to some processes surrounding the rod bipolar cell terminals, which are AGB immunonegative (Fig. 3B). Thus, the only bipolar cells that are labeled strongly by KA activation in the rabbit retina appear to be OFF-center cone bipolar cells, and the only completely unresponsive cells are rod bipolar cells. Attempts to activate AGB permeation of ON-center cone bipolar or rod bipolar cells through a cyclic nucleotide-gated channel by elevating isobutylmethylxanthine or by applying exogenous, permeant cyclic GMP analogues were unsuccessful.

KA activation in the amacrine cell layer

Although it is not possible to uniquely classify every amacrine cell type with amino acid immunocytochemistry, virtually all amacrine cells display GABA- or glycine-dominated signatures (Marc et al., 1995; Kalloniatis et al., 1996). GABA- and glycine-positive amacrine cells displayed a range of KA-activated AGB signals (Fig. 4). Some

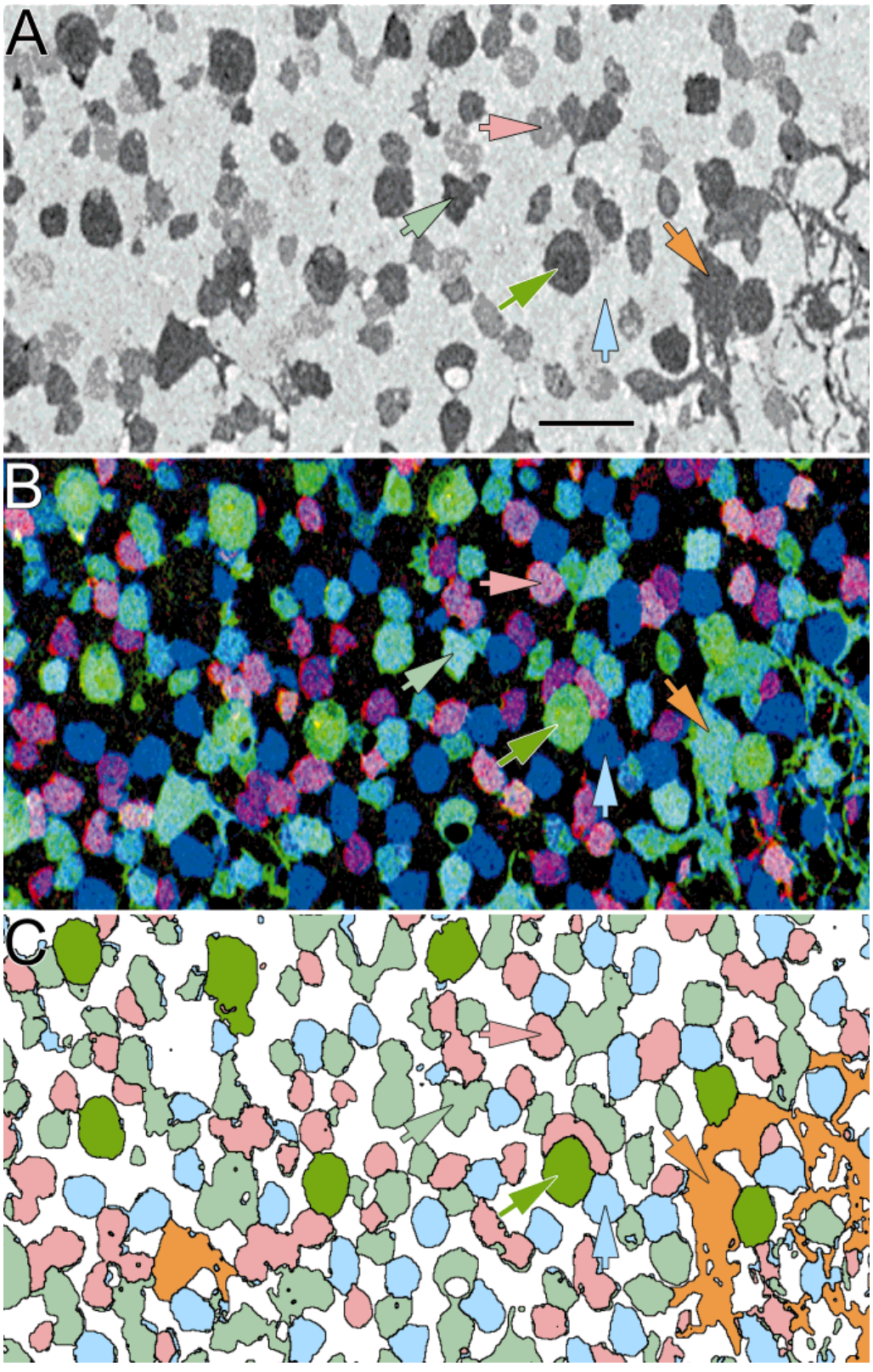

Figure 1

GABA-positive cells were strongly activated by KA, whereas some equally GABA-immunoreactive cells displayed very weak AGB signals (Fig. 4A,C). All glycine-positive cells showed moderate to strong responses to KA activation (Fig. 4B,C). Some resolution of these populations can be achieved with GABA · AGB · glycine → rgb mapping (Fig. 5A) and pattern recognition (Fig. 5B). Even with single-dose KA activation, it is possible to separate the amacrine cell layer into seven statistical classes (Fig. 6). The GABA-positive population is complex, with at least three statistically significant classes ($P_e \leq 0.05$), each of which has a broad response histogram indicative of the existence of cellular subtypes in each class expressing functionally different AMPA/KA receptors. Two statistically separable ($P_e \leq 0.01$) classes of glycine-positive amacrine cells are present in this sample of retina. One of those classes possesses a uniform soma size and pattern with a conformity ratio of 2.5 ($n = 60$; $P < 0.01$) and perhaps represents rabbit A_{II} amacrine cell (Mills and Massey, 1991). Two remaining groups, classes 6 and 7, likely represent OFF-center and rod bipolar cells, with the possible inclusion of some amacrine cell types that have lost too much of their transmitter signal to be classified (Murry and Marc, 1995).

KA activation in the ganglion cell layer

The ganglion cell layer of the rabbit retina contains both ganglion and amacrine cells (Vaney and Hughes, 1976; Vaney, 1980; Hughes, 1985; Peichl et al., 1987; Amthor et al., 1989a,b), subsets of which posses signatures that can be classified by pattern recognition (Marc et al., 1995; Kalloniatis et al., 1996). Figure 7A displays neurons in the ganglion cell layer after exposure to 6 μM KA with GABA · AGB · glutamate → *rgb* mapping. The combination of strong red GABA signals and strong green AGB signals produced an array of bright yellow cells of similar morphology. Conversely, many pure blue glutamate-positive cells and magenta glutamate- and GABA-positive cells lacked any significant AGB signal. Certain large cells demonstrated weak AGB responses to KA and, thus, appeared tinted cyan. The cells in Figure 7A represent a set of 228 neurons that can be grouped by pattern recognition into five statistically separable classes with distinctive biochemical signatures (Fig. 8), populations, and sizes (Table 1). After activation with 63 μM KA (Figs. 7B, 8), many more cells display strong AGB signals, with some interesting exceptions. Class 1 cells are large to medium-sized glutamate-positive cells, likely including α ganglion cells (Peichl et al., 1987), which express modest responses at low KA doses but are the most KA sensitive of ganglion cells. Small to medium-sized class 2 cells lack responsiveness to low KA doses and exhibit weak-to-moderate responses at high doses. Because classification is based solely on biochemical signatures, the distinctiveness of class 2 cells is secured further by the fact that they are smaller than class 1 cells, with $P \leq 0.01$ (Table 1). Class 3 cells represent the presumed GABA-positive ganglion cells of the rabbit retina (Yu et al., 1988) but may include unidentified amacrine cell types, lacking low-dose KA responses but appearing biochemically and morphologically complex. Class 3 cells exhibit substantial signal

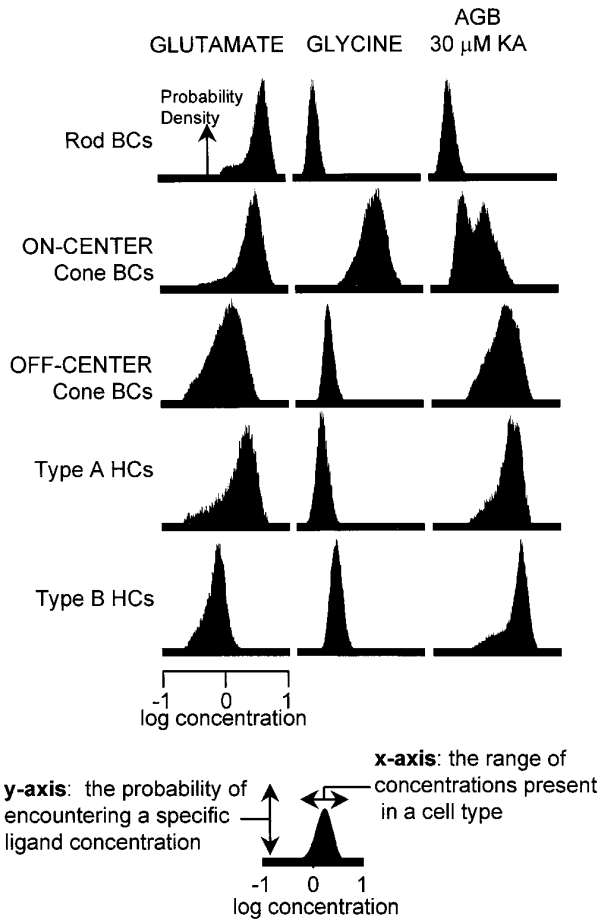

Fig. 2. Probability-density histograms of bipolar cells (BCs) and horizontal cells (HCs) derived from pattern recognition. Each column represents the histogram for one signal (glutamate, glycine, or AGB in the presence 30 μM KA), and each row represents the signature for each class. The y-axis of each histogram is the peak normalized probability of encountering a given signal concentration, and the x-axis represents the range of detectable intracellular concentrations (log mM). Histogram alignment on the x-axis indicates the concentration range for that cell type. All classes were separable with a probability of error (P_e) of <0.01.

Fig. 1. Bipolar and horizontal cell responses to 30 μM kainate (KA). **A:** 1-Amino-4-guanidobutane (AGB) immunoreactivity in a 250-nm section through the distal half of the inner nuclear layer after activation by 30 μM KA. Five kinds of cells are indicated by arrows in A–C: The pale blue vertical arrow indicates a nonresponsive area that is actually the soma of a rod bipolar cell, the pale red horizontal arrow indicates a weakly responsive ON-center cone bipolar cell, the oblique downward orange arrow indicates a type A horizontal cell, and the pale and dark green upward oblique arrows indicate an OFF-center bipolar and a type B horizontal cell, respectively. **B:** Glycine · AGB · glutamate → red-green-blue (rgb) mapping of three serial 250-nm horizontal sections, including the section shown in A. Arrows, as in A, reveal the pure blue glutamate signal of rod bipolar cells, the reddish glycine-rich signal of ON-center cone bipolar cells, and the green AGB-rich signals of OFF-center bipolar cells and horizontal cells. **C:** A theme map based on a K-means classification of these signals (plus glutamine and glutathione signals) defines five cell classes: white, Müller cells; pale red, ON-center cone bipolar cells; pale green, OFF-center cone bipolar cells; pale blue, rod bipolar cells; dark green, type B horizontal cells; orange, type A horizontal cells. Scale bar = 20 μm.

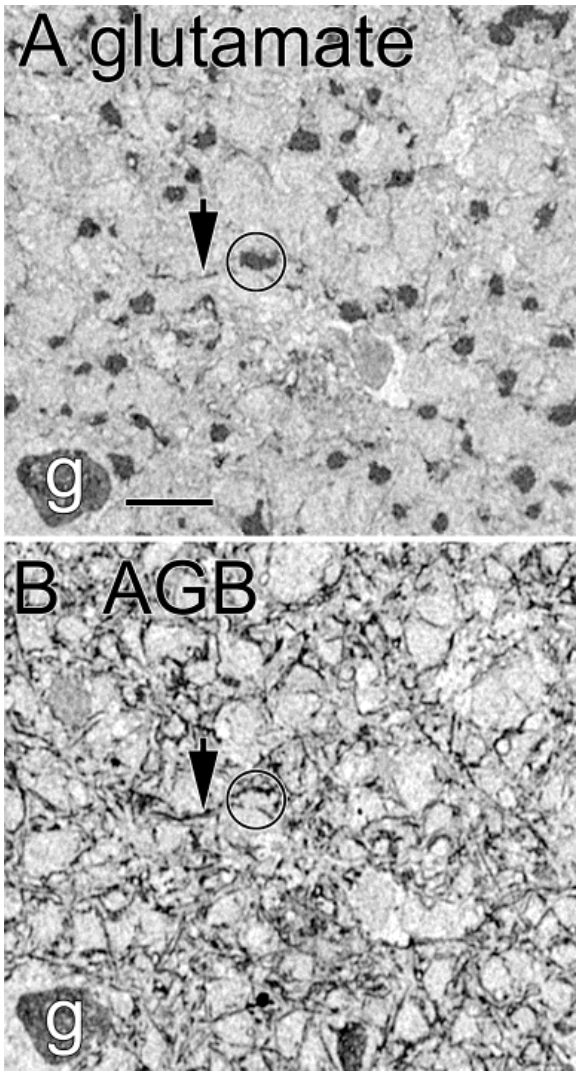

Fig. 3. Evidence for the lack of KA responses in rod bipolar cells. Serial horizontal 250-nm sections through the proximal inner plexiform layer were viewed as registered, density-scaled glutamate (**A**) and AGB (**B**) signals in response to 30 μM KA. A single rod bipolar cell terminal in the glutamate-immunoreactive array of rod bipolar cell terminals is circled in both A and B. No rod bipolar cell terminal shows any AGB signal. A ganglion cell soma (g) barely protrudes into the proximal inner plexiform layer. The arrows indicate fine ganglion cell dendrites that show responses to 30 μM KA, validating the ability of registration to capture detail. Scale bar = 12.6 μm.

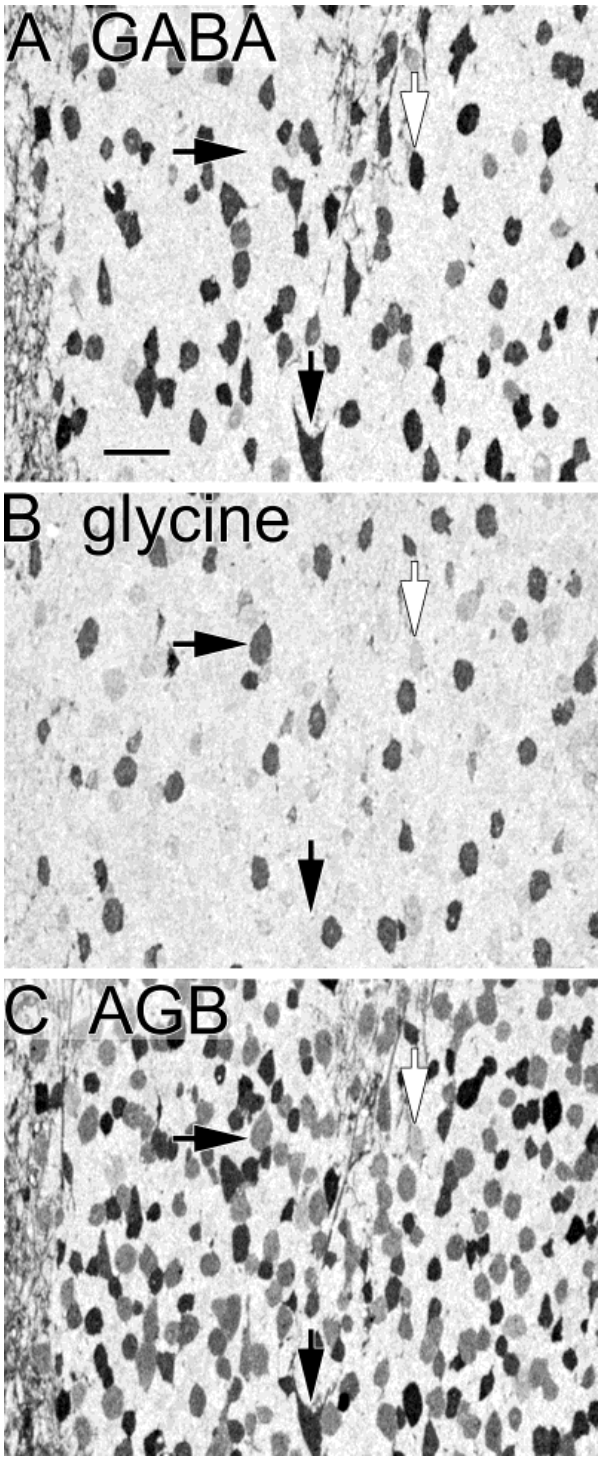

Fig. 4. Amacrine cell responses to 30 μM KA. **A:** γ-Aminobutyric acid (GABA) signals from one of three serial 250-nm horizontal sections centered on the amacrine cell layer (a portion of the inner plexiform layer protrudes into the field at the left border and at upper right center in A–C). Two strongly GABA-positive cells (downward black and white arrows) and one GABA-negative cell (horizontal black arrow) are indicated in A–C. **B:** Glycine signals reveal a unique, strong signal in a subpopulation of amacrine cells. **C:** AGB signals are strong yet vary across cell types. The white arrow indicates a weakly-responsive GABA-positive amacrine cell, and the black arrows denote distinct AGB signals after activation with 30 μM KA. Scale bar = 20 μm.

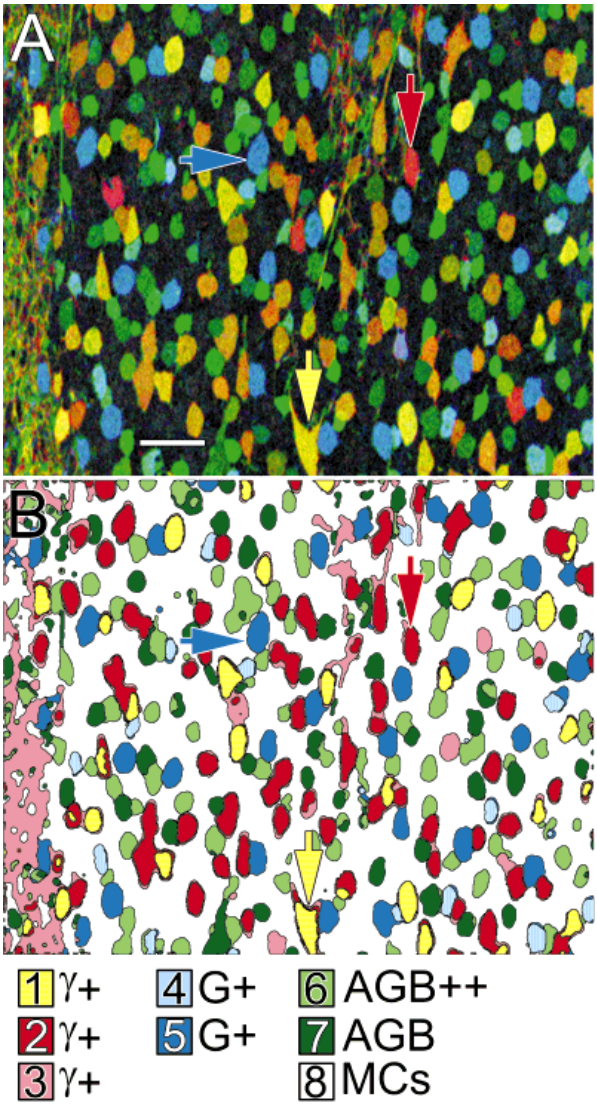

Fig. 5. Amacrine cell responses to 30 μM KA. **A:** GABA · AGB · glycine → rgb mapping of the images shown in Figure 4. Multiple hue classes of cell somata are evident against a black glial background, and apparent patterns of some individual cell types can be discerned (see text). **B:** A theme map based on a K-means classification of these signals defines eight cell classes (the code is shown at the bottom). Scale bar = 20 μm.

dispersion at higher KA doses. Starburst amacrine cells form class 4 and are the most KA sensitive of all cells in the ganglion cell layer. A sparse set of GABA-positive ovoid cells (class 5) lacked responses at 6 μM KA, and this was the only means by which they could be distinguished statistically.

DISCUSSION

KA responses of horizontal cells

There are three types of horizontal cell elements in the rabbit retina: the somata of cone-driven type A (axonless) and type B (axon bearing) horizontal cell somata and the rod-driven type B horizontal cell axon terminal arbors (Dacheux and Raviola, 1982). Both somatic types are labeled similarly by AGB after KA activation (Fig. 1), and their responses are very homogeneous. The data presented here do not resolve the responses of axon terminals. Each horizontal cell type in rabbit retina seems similar pharmacologically (Massey and Miller, 1987), and the somata of type A and type B have similar AMPA/KA thresholds (Marc, 1999) and similar responses to 30 μM KA (Figs. 1, 2). Horizontal cells are known to express subunits for both AMPA (Qin and Pourcho, 1996) and glutamate receptor (GluR) 6/7 KA subunits (Morigawa et al., 1995; Brandstätter et al., 1997, 1994), suggesting that their postsynaptic responses will have a complex pharmacology and that they should respond strongly to both AMPA and KA. In fact, horizontal cells do respond to AMPA more strongly than bipolar cells (Marc, 1999), which indicates that KA receptors may play a more powerful role in the endogenous glutamate responsivities of horizontal cells, even though some KA receptor subunits also have been found in bipolar cells (Brandstätter et al., 1997). However, because KA desensitizes true KA receptors, evidence of the unique properties of horizontal cell glutamate receptors is not available from these responses alone.

KA responses of bipolar cells

There are three types of mammalian bipolar cells: rod bipolar cells, ON-center cone bipolar cells, and OFF-center cone bipolar cells (Wässle and Boycott, 1991). Pattern recognition of endogenous amino acid signals in the mammalian retina reveals only two biochemical classes of bipolar cells, and it is known that one of those classes is a mixture of rod and OFF-center cone bipolar cells (Kalloniatis et al., 1996; Marc et al., 1999). However, AGB visualization adds another dimension of separability based on glutamatergic drive, yielding three distinct bipolar cell populations. Mixed patterns of bipolar cell responses were induced by KA (Figs. 1, 2), as expected from electrophysiologic data showing that OFF-center bipolar cells preferentially bear classical ionotropic GluRs and are KA sensitive, whereas ON-center bipolar cells employ metabotropic GluRs and are predominantly KA insensitive (Slaughter and Miller, 1981, 1983; Karschin and Wässle, 1990; Yamashita and Wässle, 1991; de la Villa et al., 1995; Euler et al., 1996; Hartveit, 1996, 1997; Sasaki and Kaneko, 1996). The responses of OFF-center bipolar cells are strong and show more dispersion than horizontal cells. The AGB histogram half-widths were 0.5, 0.3, and 0.2 log units for OFF-center bipolar cells, type A horizontal cells, and type B horizontal cells, respectively. This suggests that not all OFF-center bipolar cells have identical responses and that they likely vary in AMPA/KA receptor types.

Weak but significant AGB signals were induced in ON-center cone bipolar cells by KA, which is at variance with most prior physiologic data. However, most in situ KA responsivities of ON-center cone bipolar cells have been analyzed in amphibian retinas (see, e.g., Hensley et al., 1993), whereas data from mammalian retinas usually are from isolated cells and/or rod bipolar cells. The KA-evoked responses reported here imply that KA should evoke small currents in mammalian ON-center cone bipolar cells, perhaps due to small numbers of AMPA/KA receptors on these cells or, more plausibly, indirect depolarization through coupling with A_{II} amacrine cells that have distinc-

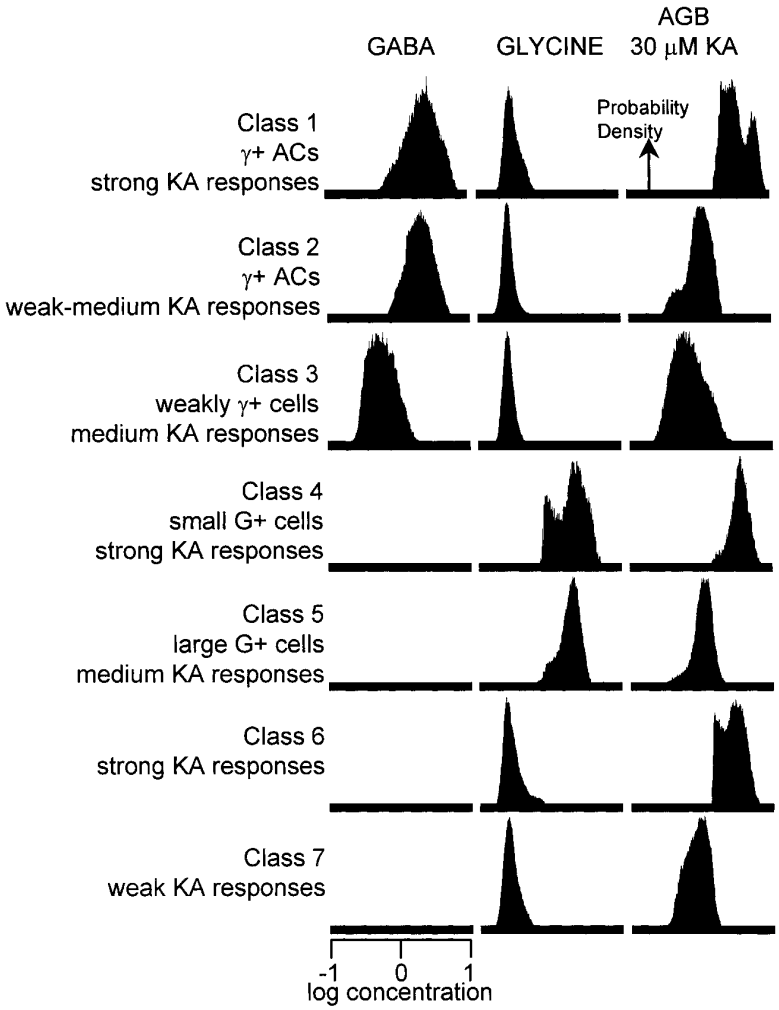

Fig. 6. Amacrine cell probability-density histograms derived from pattern recognition. Seven cell classes were separable with $P_e \leq 0.01$ except for classes 1–3, which were separable from one another at $P_e \leq 0.05$ and from classes 4–7 at $P_e \leq 0.01$. Class 1 cells were GABA-positive (γ^+) amacrine cells (ACs) with strong but clearly multimodal responses to KA, class 2 cells had weaker responses, and class 3 cells had extremely weak responses. All glycine-positive (G^+) cells (classes 4 and 5) had good responses to KA, but the two classes were clearly separable. Small, KA-responsive and unresponsive cells were derived partly from bipolar cells positioned deep in the inner nuclear layer but may also have included small amacrine cells that were depleted of neurotransmitter by KA-evoked efflux. MC.

tive KA responses (Boos et al., 1993). Hartveit (1997) recently reported that rat ON-center cone bipolar cells possess KA-activated currents and similarly concluded that they arose indirectly through coupling with A_{II} amacrine cells. The AGB signals of ON-center cone bipolar cells were distinctly bimodal. If the entire AGB signal in ON-center cone bipolar cells arises from coupling leakage, then different ON-center cells must possess different coupling efficacies (see Cohen and Sterling, 1986).

Rod bipolar cells show no AMPA/KA-activated AGB entry under any circumstances, consistent with most physiologic reports (Hartveit, 1996). Inconsistent instances of KA activate currents have been observed in rod bipolar cells, however (Karschin and Wässle, 1990). Hughes and colleagues (Hughes et al., 1992; Hughes, 1997) have reported expression of the GluR2-long flop variant subunit in mouse rod bipolar cells. The relative permeability of AGB through receptor assemblies incorporating GluR2(R) edited subunits is unknown, but the incorporation of a single edited GluR2(R) subunit into an assembly substantially attenuates Ca^{2+} permeability (Gieger et al., 1995; Washburn et al., 1997) and decreases unitary conductance (Swanson et al., 1997). Thus, the presence of edited GluR2(R) is perhaps one type of AMPA receptor variation expected to block AGB permeation and to display small currents when it is present. The role of such an ionotropic receptor on rod bipolar cells remains mysterious.

KA responses of amacrine cells

There are large numbers of amacrine cell types in the mammalian retina (Vaney, 1990), but most displayed strong KA-induced AGB signals. GABA-positive cells reflect a continuum of cell types that range from highly responsive to relatively unresponsive, the latter being few

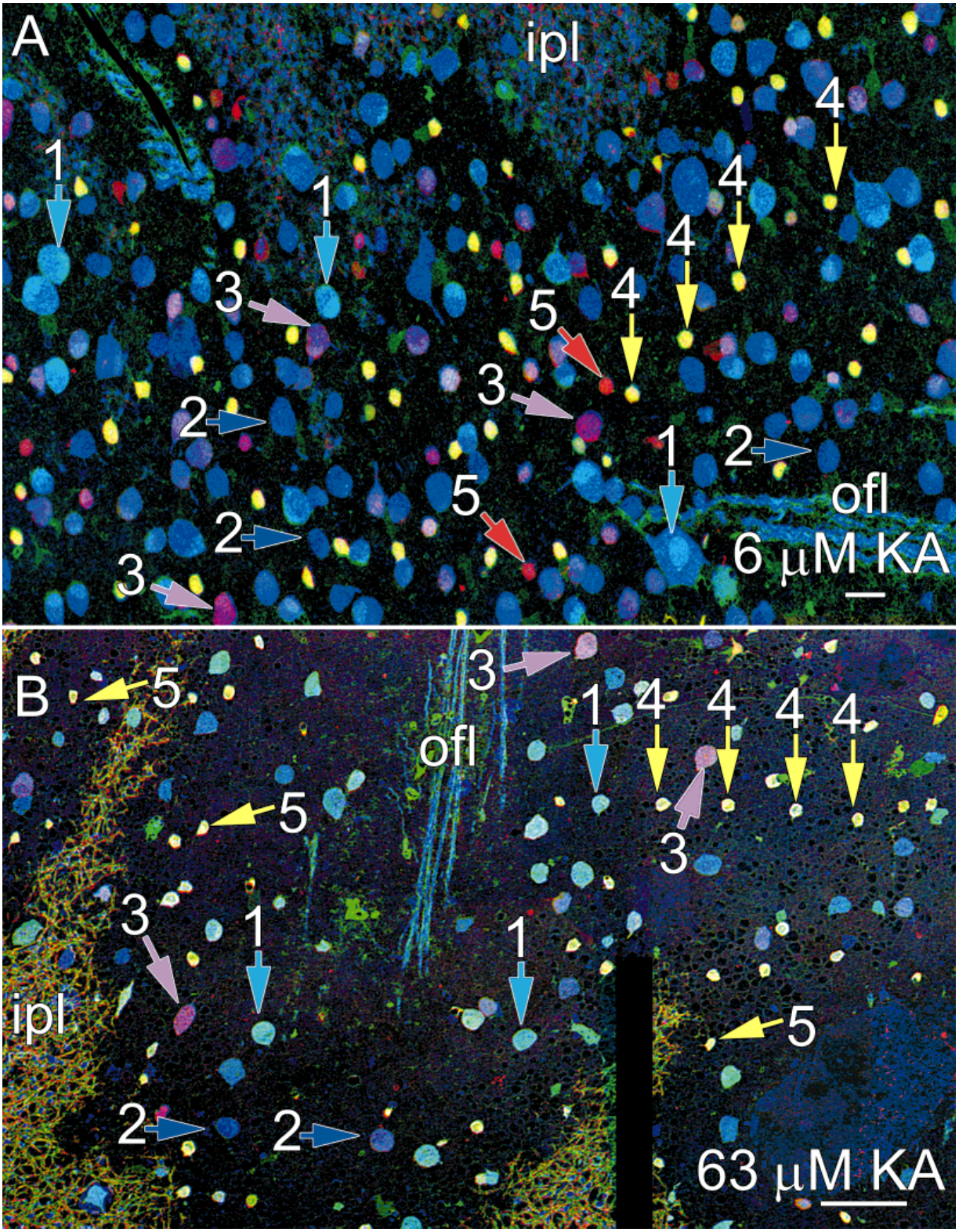

Fig. 7. Responses of neurons in the ganglion cell layer to KA. **A:** Responses to 6 μM KA viewed as a GABA · AGB · glutamate → rgb map of three registered serial 250-nm sections. This low dose of KA preferentially activates GABA-positive starburst amacrine cells (bright yellow; class 4), whereas other cell types are either unresponsive (classes 2, 3, and 5) or have weak responses (class 1). **B:** Responses to 63 μM KA viewed as AGB immunoreactivity. A variety of response strengths is present, including strong responses from class 1 cells (bright cyan) and class 4 cells (yellow). Even at this dose of KA, some ganglion cells (classes 2 and 3) fail to generate strong signals. ipl, Inner plexiform layer; ofl, optic fiber layer. Scale bars = 20 μm in A, 50 μm in B.

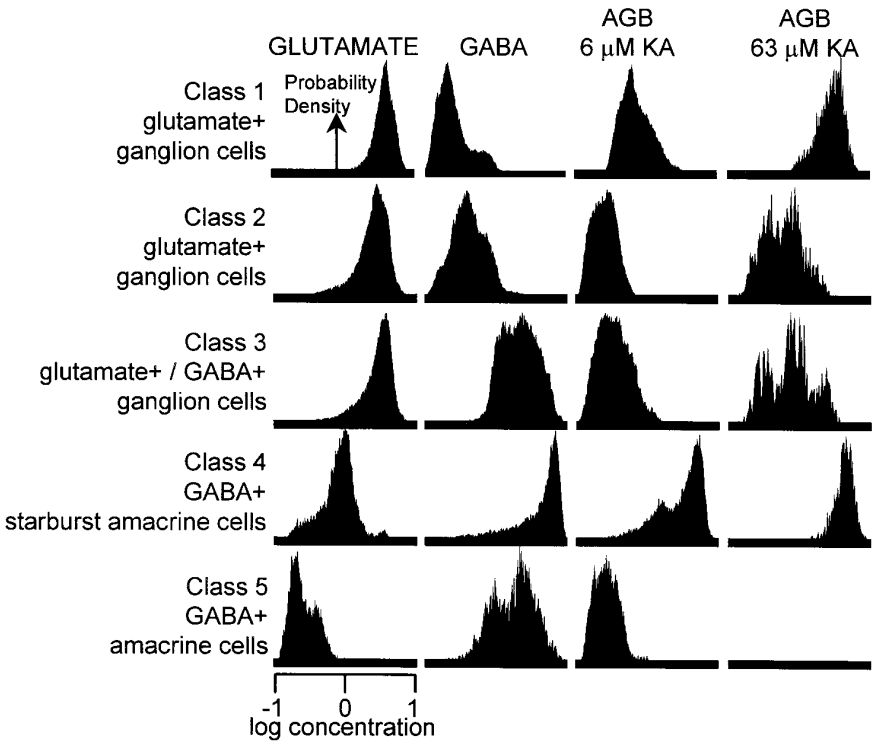

Fig. 8. Ganglion cell layer probability-density histograms derived from pattern recognition, inclusive of over 200 cells each for the 6-μM and 63-μM response columns, respectively. Note that the class 4 (starburst amacrine cell) histogram reveals stronger responses than any other cell type at 6 μM KA. Class 1 cells have weak 6-μM responses but strong 63-μM responses. Class 2 and class 3 cells are poorly responsive at low doses and reveal complex response patterns at high doses. AGB signals were not discriminated for class 5 amacrine cells at 63 μM KA.

TABLE 1. Summary Properties of Neurons in the Rabbit Ganglion Cell Layer

	Class[1]				
Measure	1	2	3	4	5
Characteristic signature	Glutamate+	Glutamate+	Glutamate+, GABA+	GABA+	GABA+
Absolute KA sensitivity scaled as 1–5 (high to low)	2	4	3	1	5
High-dose KA responsivity scaled as 1–5 (high to low)	2	3–4	3–4	1	1
Percent of cells in the ganglion cell layer (midinferior retina)	22	26	32	12	8
Diameter mean ± S.D. (μm; not corrected for shrinkage)	13.5 ± 4.4	11.4 ± 2.6	10.7 ± 2.4	8.6 ± 0.6	8.7 ± 1.4
Diameter significantly different from other classes ($P < 0.01$; Student's t-test)	2, 3, 4, 5	1, 4, 5	1, 4, 5	1, 2, 3	1, 2, 3
Probable ganglion cell (GC) or amacrine cell (AC) types	α and other GCs	Mixed GCs	Mixed GABA+ GCs	Starburst ACs	GABA+ ACs

[1]KA, kainate; GABA, γ-aminobutyric acid; +, positive.

in number. This is consistent with the evidence that dopaminergic cells are the only amacrine cells established to be resistant to KA excitotoxicity (Morgan, 1983), and they represent one of the least numerous cell types. Furthermore, mammalian dopaminergic neurons are GABA positive (Wülle and Wagner, 1990). Although the lack of AGB signals in this set of GABA-positive amacrine cells could be due to the presence of AGB-impermeant forms of AMPA receptors (see below), it is better explained by the existence of a cell type that lacks significant numbers of AMPA/KA receptors. The glycine-positive amacrine cell group was completely KA responsive, with one group of small cells showing the greatest responsivity and a class similar to A_{II} amacrine cells in size, distribution, and conformity ratio, displaying weaker but distinct responses. The mean response magnitude of this class of glycine-positive amacrine cells was identical to that of the stronger response mode of ON-center cone bipolar cells, as expected if effective coupling between the two types allowed rapid intercellular equilibration of AGB.

In the amacrine cell and ganglion cell layers, the responses of starburst amacrine cell s were evident in both KA- and AMPA-activated preparations (Marc, 1999). Identification of class 4 cells as cholinergic cells, per se, is not possible, because AGB and choline acetyltransferase immunocytochemistry are incompatible. However, such a correspondence is not required to make a robust identification. The displaced starburst amacrine cells are the largest population of GABA-positive cells in the ganglion cell layer (Vaney and Young, 1988), as are class 4 cells. This alone is

sufficient to assert that they are starburst amacrine cells, but the correspondence is bolstered by additional evidence. Class 4 cells arborize at inner plexiform layer level 70, and their counterparts in the amacrine cell layer arborize at level 20, identical to values for rabbit starburst amacrine cells (Brandon, 1987a,b). They form a nonrandom array with a conformity ratio of 2.9 ($n = 75$; $P < 0.0001$), which is statistically indistinguishable from the conformity ratio of dye-injected starburst amacrine cells (conformity ratio = 3.1; Masland et al., 1984). Their distributions, proportions, and sizes match those determined from choline acetyltransferase, glutamate decarboxylase, and GABA immunoreactivity as well as from neurofibrillar staining (Vaney et al., 1981; Brandon, 1987a,b; Brecha et al., 1988; Vaney and Young, 1988). Thus, it is not surprising that the sensitivity of starburst amacrine cells determined by AGB mapping (Marc, 1999) matches that determined for [^{14}C] acetylcholine release (Linn et al., 1991). Other than a single type of OFF-center bipolar cell with unique channel properties that are not discussed in this paper, starburst amacrine cells appear to be the most KA sensitive cell in the retina.

KA responses of ganglion cells

Most, but not all, ganglion cells exhibit strong KA-activated AGB signals. However, Massey and Miller (1988) reported that all units in a large sample of rabbit retinal ganglion cells were KA responsive. Similarly, all cat α and β cells (Cohen et al., 1994) and nearly all primate retinal ganglion cells (Cohen and Miller, 1994; Zhou et al., 1994) are KA responsive with quinoxaline block of those responses. The limitation of these physiologic reports is the absence of quantitative comparisons across ganglion cell types. In contrast, the AGB mapping method reveals different degrees of responsivity across neighboring cells in the ganglion cell layer, arguing that trigger features of ganglion cells are derived in part from different types of AMPA/KA receptors. Class 2 ganglion cells (Figs. 7, 8) exhibit weak KA-activated AGB signals and are quite common. Unlike bipolar and amacrine cells, no ganglion cell types have been characterized previously as lacking AMPA/KA receptors. One explanation of this difference could be that all ganglion cells use AMPA receptors but that AGB may not permeate all types of AMPA-gated channels effectively. AMPA receptors comprised of subunits GluR1, GluR3, and GluR4 exhibit substantial Ca^{2+} permeability, whereas inclusion of the edited GluR2(R) subunit in any AMPA receptor complex leads to diminution of Ca^{2+} permeability and single-channel conductance (for reviews, see Hollman and Heinemann, 1994; Burnashev, 1996; Swanson et al., 1997; Washburn et al., 1997). The GluR2(R) subunit similarly may restrict entry by AGB. Consistent with this, GluR2 mRNA signals are abundant in the inner nuclear and ganglion cell layers of the rat retina (Hughes et al., 1992; Müller et al., 1992). Alternatively, some class 2 ganglion cells could have a paucity of AMPA receptors, with substitution of KA receptors as the fast ionotropic mechanism and KA receptor desensitization (Paternain et al., 1995) effecting diminished AGB entry. Regardless of the mechanism underlying restriction of AGB entry, the overall properties of the AMPA/KA-gated channels on different cell types of ganglion cells cannot be equivalent.

The sizes of the class 1 ganglion cells suggest that they most certainly account for α ganglion cells and could include other cells as well. Thus, class 1 ganglion cells, which are the most KA sensitive cells, certainly include some "brisk" ganglion cells. Conversely, class 2 ganglion cells are smaller, with significant within-group variability, and almost certainly includes some "sluggish" ganglion cells. One prediction of AGB mapping is that brisk and sluggish ganglion cells will have distinctly different KA thresholds and, consequently, different thresholds for the endogenous ligand glutamate. Class 3 GABA-positive cells have never been knowingly recorded physiologically, but they also show diverse responses to KA, suggesting that multiple receptor types are expressed and that there is likely more than one subtype of GABA-positive ganglion cell.

Future directions

Because KA does not desensitize at AMPA receptors, AGB mapping after KA activation provides a robust catalog of AMPA receptor distributions in the retina. However, the degree to which these same cells depend on KA receptors cannot be characterized accurately. Moreover, AMPA activation patterns are similar to those of KA but are clearly distinguishable in the strength of activation and numbers of cells activated (Marc, 1999). The use of desensitizing ligands and antagonists selective for AMPA receptors may further discriminate subtypes of OFF-center cone bipolar, amacrine, and ganglion cells, using the basic classifications established with KA activation as a reference. Similarly, patterns of NMDA activation are quite different from both AMPA and KA activation and will permit further refinement of classifications.

ACKNOWLEDGMENTS

This work was supported by a Research to Prevent Blindness Jules and Doris Stein Professorship.

LITERATURE CITED

Ames A III, Nesbett FB. 1981. In vitro retina as an experimental model of the central nervous system. J Neurochem 37:867–877.

Amthor FR, Takahashi ES, Oyster CO. 1989a. Morphologies of rabbit retinal ganglion cells with concentric receptive fields. J Comp Neurol 280:72–96.

Amthor FR, Takahashi ES, Oyster CO. 1989b. Morphologies of rabbit retinal ganglion cells with complex receptive fields. J Comp Neurol 280:97–121.

Boos R, Schneider H, Wässle H. 1993. Voltage- and transmitter-gated currents of AII-amacrine cells in a slice preparation of the rat retina. J Neurosci 13:2874–2888.

Brandon C. 1987a. Cholinergic neurons in the rabbit retina: immunocytochemical localization, and relationship to GABAergic and cholinesterase-containing neurons. Brain Res 401:385–391.

Brandon C. 1987b. Cholinergic neurons in the rabbit retina: dendritic branching and ultrastructural connectivity. Brain Res 426:119–130.

Brandstätter JH, Hartveit E, Sassoe-Pognetto M, Wässle H. 1994. Expression of NMDA and high-affinity kainate receptor subunit mRNAs in the adult rat retina. Eur J Neurosci 6:1100–1112.

Brandstätter JH, Koulen P, Wässle H. 1997. Selective synaptic distribution of kainate receptor subunits in the two plexiform layers of the rat retina. J Neurosci 17:9298–9307.

Brecha N, Johnson D, Peichl L, Wässle H. 1988. Cholinergic amacrine cells of the rabbit retina contain glutamate decarboxylase and γ-aminobutyrate immunoreactivity. Proc Natl Acad Sci USA 85:6187–6191.

Burnashev N. 1996. Calcium permeability of glutamate-gated channels in the central nervous system. Curr Opin Neurobiol 6:311–317.

Cohen ED, Miller RF. 1994. The role of NMDA and non-NMDA excitatory amino acid receptors in the functional organization of primate retinal ganglion cells. Vis Neurosci 11:317–322.

Cohen E, Sterling P. 1986. Accumulation of 3H-glycine by cone bipolar neurons in the cat retina. J Comp Neurol 250:1–7.

Cohen ED, Zhou ZJ, Fain GL. 1994. Ligand-gated currents of alpha and beta ganglion cells in the cat retinal slice. J Neurophysiol 72:1260–1269.

Cook JE. 1996. Spatial properties of retinal mosaics: an empirical evaluation of some existing measures. Vis Neurosci 13:15–30.

Dacheux RF, Raviola E. 1982. Horizontal cells in the retina of the rabbit. J Neurosci 2:1486–1493.

de la Villa P, Kurahashi T, Kaneko A. 1995. L-glutamate-induced responses and cGMP-activated channels in three subtypes of retinal bipolar cells dissociated from the cat. J Neurosci 15:3571–3582.

Euler T, Wässle H. 1995. Immuncytochemical identification of cone bipolar cells in the rat retina. J Comp Neurol 361:461–478.

Euler T, Schneider H, Wässle H. 1996. Glutamate responses of bipolar cells in a slice preparation of the rat retina. J Neurosci 16:2934–2944.

Famiglietti EV. 1981. Functional architecture of cone bipolar cells in the mammalian retina. Vision Res 21:1559–1563.

Gieger JRP, Melcher T, Koh D-S, Sakmann B, Seeburg PH, Jonas P, Monyer H. 1995. Relative abundance of subunit mRNAs determines gating and Ca^{2+} permeability of AMPA receptors in principal neurons and interneurons of rat CNS. Neuron 15:193–204.

Hartveit E. 1996. Membrane currents evoked by ionotropic glutamate receptor agonists in rod bipolar cells in the rat retinal slice preparation. J Neurophysiol 76:401–422.

Hartveit E. 1997. Functional organization of cone bipolar cells in the rat retina. J Neurophysiol 77:1716–1730.

Hensley SH, Yang X-L, Wu SM. 1993. Identification of glutamate receptor subtypes mediating inputs to bipolar cells and ganglion cells in the tiger salamander retina. J Neurophysiol 69:2099–2107.

Hollman M, Heinemann S. 1994. Cloned glutamate receptors. Annu Rev Neurosci 17:31–108.

Hughes A. 1985. New perspectives in retinal organisation. Progr Retinal Res 4:243–313.

Hughes TE. 1997. Are there ionotropic glutamate receptors on the rod bipolar cell of the mouse retina? Vis Neurosci 14:103–109.

Hughes TE, Hermans-Borgmeyer I, Heinemann S. 1992. Differential expression of glutamate receptor genes (GluR 1–5) in the rat retina. Vis Neurosci 8:49–55.

Kalloniatis M, Marc RE, Murry RF. 1996. Amino acid signatures in the primate retina. J Neurosci 16:6807–6829.

Karschin A, Wässle H. 1990. Voltage- and transmitter-gated currents in isolated rod bipolar cells of rat retina. J Neurophysiol 63:860–876.

Lerma J, Paternain AV, Naranjo JR, Mellstrm B. 1993. Functional kainate-selective glutamate receptors in cultured hippocampal neurons. Proc Natl Acad Sci USA 90:11688–11692.

Linn DM, Blazynski C, Redburn DA, Massey SC. 1991. Acetylcholine release from the rabbit retina mediated by kainate receptors. J Neurosci 11:111–122.

Marc RE. 1999. Mapping glutamatergic drive in the vertebrate retina with a channel-permeant organic cation. J Comp Neurol 407:47–64.

Marc RE, Liu W-LS. 1985. Glycine-accumulating neurons in the human retina. J Comp Neurol 232:241–260.

Marc RE, Basinger SF, Murry RF. 1995. Pattern recognition of amino acid signatures in retinal neurons. J Neurosci 15:5106–5129.

Marc RE, Murry R, Fisher SK, Linberg K, Lewis G, Kalloniatis M. 1998. Amino acid signatures in the normal cat retina. Invest Ophthalmol Vis Sci 39:1685–1693.

Masland RH, Mills JW, Hayden SA. 1984. Acetylcholine-synthesizing amacrine cells: identification and selective staining by using radioautography and fluorescent markers. Proc R Soc London B 223:79–100.

Massey SC, Miller RF. 1987. Excitatory amino acid receptors of rod- and cone-driven horizontal cells in the rabbit retina. J Neurophysiol 57:645–659.

Massey SC, Miller RF. 1988. Glutamate receptors of ganglion cells in the rabbit retina: evidence for glutamate as a bipolar cell transmitter. J Physiol 405:635–655.

Mills SL, Massey SC. 1991. Labeling and distribution of AII amacrine cells in the rabbit retina. J Comp Neurol 304:491–501.

Mills SL, Massey SC. 1992. Morphology of bipolar cells labeled by DAPI in the rabbit retina. J Comp Neurol 321:133–149.

Morgan IG. 1983. Kainic acid as a tool in retinal research. Progr Retinal Res 2:249–266.

Morigawa K, Vardi N, Sterling P. 1995. Immunostaining for glutamate receptor subunits in mammalian retina [part 2]. Soc Neurosci Abstr 21:901.

Müller F, Greferath U, Wässle H, Wisden W, Seeburg P. 1992. Glutamate receptor expression in the rat retina. Neurosci Lett 138:179–182.

Murry RF, Marc RE. 1995. Glutamatergic driving of amacrine and bipolar cell populations in the goldfish retina. Invest Ophthalmol Vis Sci 36(Suppl):S383.

Paternain AV, Morales M, Lerma J. 1995. Selective antagonism of AMPA receptors unmasks kainate receptor-mediated responses in hippocampal neurons. Neuron 14:185–189.

Peichl L, Buhl EH, Boycott BB. 1987. Alpha ganglion cells in the rabbit retina. J Comp Neurol 263:25–41.

Peng Y-W, Blackstone CD, Huganir RL, Yau KW. 1995. Distribution of glutamate receptor subtypes in the vertebrate retina. Neuroscience 66:483–497.

Pourcho R, Goebel DJ. 1987. Visualization of endogenous glycine in the cat retina: an immunocytochemical study with Fab fragments. J Neurosci 7:1189–1197.

Pow DV, Crook DK. 1995. Immunocytochemical evidence for the presence of high levels of reduced glutathione in radial glial cells and horizontal cells of the rabbit retina. Neurosci Lett 193:25–28.

Qin P, Pourcho RG. 1996. Distribution of AMPA-selective glutamate receptor subunits in cat retina. Brain Res 710:303–307.

Sasaki T, Kaneko A. 1996. L-glutamate-induced responses in OFF-type bipolar cells of the cat retina. Vision Res 36:787–795.

Slaughter MM, Miller RF. 1981. 2-Amino-4-phosphonobutyric acid: a new pharmacological tool for retina research. Science 211:182–185.

Slaughter MM, Miller RF. 1983. An excitatory amino acid antagonist blocks cone input to sign-conserving second-order retinal neurons. Science 219:1230–1232.

Strettoi E, Masland RH. 1995. The organization of the inner nuclear layer of the rabbit retina. J Neurosci 15:875–888.

Swanson GT, Kamboj SK, Cull-Candy SG. 1997. Single-channel properties of recombinant AMPA receptors depend on RNA editing, splice variation, and subunit composition. J Neurosci 17:58–69.

Vaney D. 1980. A quantitative comparison between the ganglion cell populations and axonal outflows of the visual streak and periphery of the rabbit retina. J Comp Neurol 189:215–233.

Vaney D. 1985. The morphology and topographic distribution of AII amacrine cells in the cat retina. Proc R Soc London B 224:475–488.

Vaney D. 1990. The mosaic of amacrine cells in the mammalian retina. Progr Retinal Res 9:49–100.

Vaney D, Hughes A. 1976. The rabbit optic nerve: fibre diameter spectrum, fibre count and comparison with a retinal ganglion cell count. J Comp Neurol 170:241–252.

Vaney D, Young H. 1988. GABA-like immunoreactivity in cholinergic amacrine cells of the rabbit retina. Brain Res 438:369–373.

Vaney D, Peichl L, Boycott BB. 1981. Matching populations of amacrine cells in the inner nuclear and ganglion cell layers of the rabbit retina. J Comp Neurol 199:373–391.

Washburn MS, Numberger M, Zhang S, Dingledine R. 1997. Differential dependence on GluR2 expression of three characteristic features of AMPA receptors. J Neurosci 24:9393–9406.

Wässle H, Boycott BB. 1991. Functional architecture of the mammalian retina. Physiol Rev 71:447–480.

Wässle H, Reimann HJ. 1978. The mosaic of nerve cells in the mammalian retina. Proc R Soc London B 200:441–461.

Wülle I, Wagner H-J. 1990. GABA and tyrosine hydroxylase immunocytochemistry reveal different patterns of colocalization in retinal neurons of various vertebrates. J Comp Neurol 296:173–178.

Yamashita M, Wässle H. 1991. Responses of rod bipolar cells isolated from the rat retina to the glutamate agonist 2-amino-4-phosphonobutyric acid (APB). J Neurosci 11:2372–2382.

Yu BC-Y, Watt CB, Lam DMK, Fry KR. 1988. GABAergic ganglion cells in the rabbit retina. Brain Res 439:376–382.

Zhou ZJ, Marshak DM, Fain GL. 1994. Amino acid receptors of midget and parasol ganglion cells in primate retina. Proc Natl Acad Sci USA 91:4907–4911.